7. M. Matson and J. Dozier, *Photogramm. Eng. Rem. Sensing* 47, 1311 (1981).
8. There are few weather observations available at present in this region at this time. Even the temperature sounding capability from the polar satellites may be somewhat suspect until the impact of the enhanced $CO_2$ abundances within the plume and the effects of smoke opacity are better known.
9. G. J. Tripoli, in preparation. The model used a triply nested grid with 1.5-, 4.5-, and 13.5-km resolutions. Fires were represented by a mean heat and smoke flux into a cylindrical region 750 m deep and 10 km in diameter; the heat source was taken to be 8.6 $kWm^{-2}$, a worst case estimate. It was also assumed that 100% of the smoke would be activated as cloud droplet nuclei in the event that air saturation was reached and that scavenging would occur if the smoke containing cloud droplets were collected onto a falling precipitation particle. The mean April winds used for the simulation were relatively strong, reaching 45 m $s^{-1}$ at upper levels. The observed convective cloud system seen in Fig. 3 similarly developed in a conditionally unstable environment as the sun rose in the sky and a low-level pressure trough could be seen traversing over the area. While the ambient upper level flow from the northwest could be clearly seen, the cloud was seen to grow over the fires in late afternoon and eventually emit a circular ring as seen in this late-stage image.
10. The METEOSAT and NOAA-10 digital data were received at the Space Science and Engineering Center of the University of Wisconsin–Madison. Cooperation of many individuals in gathering and analysis of these data is gratefully acknowledged. Discussions with F. Bretherton, D. W. Martin, L. A. Sromovsky, J. Kutzbach, and H. S. Limaye have been particularly useful. Finally, we thank two anonymous referees for their comments.

21 March 1991; accepted 1 May 1991

---

# $^{40}Ar/^{39}Ar$ Age of Cretaceous-Tertiary Boundary Tektites from Haiti

G. A. Izett, G. B. Dalrymple, L. W. Snee

**$^{40}Ar/^{39}Ar$ dating of tektites discovered recently in Cretaceous-Tertiary (K-T) boundary marine sedimentary rocks on Haiti indicates that the K-T boundary and impact event are coeval at 64.5 ± 0.1 million years ago. Sanidine from a bentonite that lies directly above the K-T boundary in continental, coal-bearing, sedimentary rocks of Montana was also dated and has a $^{40}Ar/^{39}Ar$ age of 64.6 ± 0.2 million years ago, which is indistinguishable statistically from the age of the tektites.**

THE DISCOVERY OF RELIC TEKTITES (*1, 2*) in K-T boundary rocks near Beloc, Haiti, has opened the door for geochemical studies needed for an understanding of K-T boundary phenomena, including the isotopic dating of these unusual objects. Tektites are glass-melt droplets formed by the instantaneous fusion of terrestrial rocks during large-scale hypervelocity impact events (*3*). The Haitian tektites are similar in composition and morphology to other classes of tektites (*1*), but their stratigraphic position and our new isotopic ages show that they are nearly twice as old as North American tektites [35.4 and 35.5 million years ago (Ma)], which were the oldest tektites known (*4*).

For the past 30 years, the goal of numerous isotopic studies has been to obtain an accurate age for the K-T boundary. This goal assumed new importance after an Ir anomaly (*5*) and shock-metamorphosed quartz grains were discovered (*6*) in K-T boundary rocks worldwide, indicating that one, or possibly several, large asteroids or comets struck Earth at the end of the Cretaceous Period. Particular efforts have been made to date minerals in bentonite (altered volcanic ash) beds that occur in coal-bearing nonmarine sedimentary rocks 1 to 21 m above the K-T boundary in western North America (*7–9*). These studies have established ages that range from 63.5 to 66.0 Ma for nonmarine rocks, but the isotopic age of marine rocks, which also record the K-T impact event at numerous sites worldwide (*5, 6*), had not been determined. To fill this gap in knowledge, we report $^{40}Ar/^{39}Ar$ ages for the Haitian tektites and, for control and correlation, for sanidine crystals from nonmarine bentonite (HC bentonite) in the Z coal bed that lies directly above the K-T boundary in the Hell Creek area of Montana (*9*).

The Haitian tektites occur together with an Ir abundance anomaly (2.3 ppb) and shock-metamorphosed quartz grains in a marl bed 0.5 m thick that marks the paleontologic K-T boundary (*1, 10*). This marl bed is in the lower part of the Beloc Formation, a sequence 150 m thick of marine limestone (*11*).

A remarkable feature of this bed is its content of numerous clay pellets, and about 2% of the pellets in the lower 2 cm of the bed contain relic tektites (*1*). The pellets occur throughout the bed, but they are most abundant (~60%) near its base (*1*). A typical tektite-bearing clay pellet consists of a corroded glass core enclosed within a jacket or shell of iron-rich smectite. The smectite shell is the alteration product of the glass. Many pellets are hollow and others are solid. About 75% have irregular, rounded shapes, but the remaining 25% have shapes typical of tektites (*12*), including spheroids, discoids, spindles, teardrops, rods, and dumbbells. Spherical pellets vary from 0.5 to 3.5 mm in diameter; dumbbells, teardrops, spindles, and irregular-shaped objects range from 3 to 10 mm in length. In 1980, these pellets were referred to as possible microtektites by Maurrasse (*13*) and 10 years later as altered tektites by Hildebrand and Boynton (*10*).

In reflected light, most tektites are dark brown to black, but in transmitted light they range from pale brown to pale yellowish brown (Fig. 1). Rare tektites have a golden honey color. Some contain spherical (common) and almond-shaped (less common) bubbles, but all lack microlites and crystallites characteristically found in volcanic glass such as obsidian. The presence of glass in the smectite pellets, some of which have shapes identical to tektites, confirms that they are pseudomorphs of tektites (*1*). We refer below to the glass cores simply as tektites.

The major element chemical composition of the Haitian tektites (*1, 2*) is broadly similar to that of other tektite groups (*4*), except that the Haitian tektites have lower $SiO_2$ content (mean, 64%; range, 52 to 68%) and higher Fe, Ca, and Na contents. The K content of the tektites is adequate for $^{40}Ar/^{39}Ar$ dating (average, 1.2%; range, 0.7 to 1.5%).

The honey-colored tektites have extraordinarily high amounts of Ca and S (25% CaO and 0.4% S) for natural glasses (*14*). The high content of these elements suggests that some of the target materials melted during the K-T impact may have been marine rocks rich in $CaSO_4$. Beds of anhydrite have been identified in the subsurface at a candidate impact site (Chicxulub) on the Yucatan platform (*15, 16*). The anomalously high content of S and the S isotopic com-

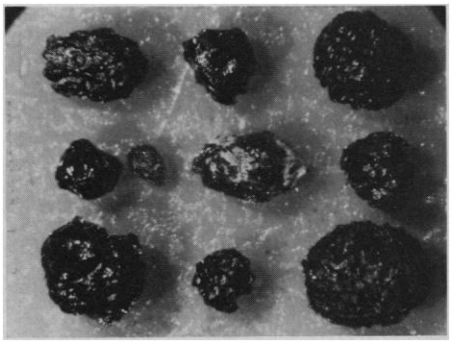

**Fig. 1.** Remnant glass cores of ten tektites from the K-T boundary marker bed on Haiti showing typical corroded surfaces. Some smectite remains on the sulfur-rich tektite near the center. The tektite in the lower right corner 1.8 mm long.

---

G. A. Izett and L. W. Snee, U.S. Geological Survey, Mail Stop 913, Denver Federal Center, Denver, CO 80225.
G. B. Dalrymple, U.S. Geological Survey, Mail Stop 937, 345 Middlefield Road, Menlo Park, CA 94025.

**Table 1.** Summary of $^{40}Ar/^{39}Ar$ incremental heating results on K-T tektites from Haiti.

| Sample* | Weight (mg) | Plateau | | Isochron | |
|---|---|---|---|---|---|
| | | $^{39}Ar$ (% [steps]) | Age† (Ma) | Age (Ma) | SUMS/($n$ − 2) |
| 90G15K-1 | 0.870 | 95.9 [15 of 25] | 64.36 ± 0.36 | 64.00 ± 0.45 | 0.32 |
| -2 | 1.117 | 98.2 [12 of 15] | 64.45 ± 0.35 | 64.25 ± 0.34 | 0.16 |
| -3 | 1.240 | 97.5 [13 of 15] | 64.35 ± 0.35 | 64.27 ± 0.33 | 0.16 |
| -4 | 1.082 | 96.9 [11 of 13] | 64.35 ± 0.35 | 64.30 ± 0.34 | 0.10 |
| 90G15L | 67.3 | 56.5 [4 of 13] | 64.8 ± 0.7 | | |

*Data for 90G15K obtained with laser system and for 90G15L with resistance furnace system. For consistency, the age of 90G15L has been normalized to a value of 513.9 Ma for MMhb-1 (see text). †Weighted mean plateau age and standard error; weighting by inverse of variance.

position (not yet determined) in the Haitian tektites may provide a strong geochemical link to the rocks of the Chicxulub structure.

Material prepared for $^{40}Ar/^{39}Ar$ dating included hand-picked tektites and sanidine crystals from the HC bentonite (*17*). Previously, minerals from this bentonite have been dated by the K-Ar, $^{40}Ar/^{39}Ar$, Rb-Sr, and U-Pb methods, with results ranging from about 63.5 to 66.0 Ma (*7–9*).

Several hundred tektites (0.3 to 4.5 mm) were extracted from a slab of the K-T marker bed for dating. They were scrubbed ultrasonically in dilute HF (~5%) for removal of all the adhering clay and then washed in distilled water. From this group, 32 tektites were selected that had the optimum size for total-fusion and incremental-heating $^{40}Ar/^{39}Ar$ dating. Most were equant, varied from 0.7 to 1.2 mm in size, and weighed about 0.3 to 1.2 mg.

The procedures used to irradiate the tektites and other samples dated are described in (*18*). The reactor fluence characteristics, irradiation procedures, and methods for measuring the corrections for interfering Ar isotopes generated by undesirable reactions with Ca and K were described in (*19*).

The calibration ages of neutron-fluence monitor minerals have a direct effect on the accuracy of $^{40}Ar/^{39}Ar$ ages calculated for unknown samples. Two of our fluence-monitor minerals, sanidine from the Fish Canyon Tuff (FCT) and hornblende (MMhb-1) from a plutonic rock in Minnesota, are used worldwide by geochronology laboratories, whereas sanidine from the Taylor Creek rhyolite (TCR) is primarily an intralaboratory standard (*20*). The ages used for these monitor minerals differ between laboratories. The U.S. Geological Survey personnel in Menlo Park, California, where most of our measurements were made, have adopted the following values: TCR, 27.92 Ma; FCT, 27.55 Ma; and MMhb-1, 513.9 Ma. These ages are based on a set of K (flame photometry) and Ar (isotope dilution) measurements made in Menlo Park on MMhb-1 and an intralaboratory biotite standard (*21*), but the Menlo Park age for MMhb-1 (513.9 Ma) is 1.26% younger than the published weighted mean of 520.4 ± 1.7 Ma (1 SE) based on measurement of K and Ar in 18 laboratories (*22*). In contrast, the ages for these fluence monitors used by U.S. Geological Survey personnel in Denver, Colorado, where one of our incremental heating measurements was made, are based on the published mean of MMhb-1 and are TCR, 28.20 Ma; FCT, 27.80 Ma; and MMhb-1, 520.4 Ma. The significance of this difference in monitor calibrations for the accuracy of the $^{40}Ar/^{39}Ar$ ages reported herein is discussed below.

The errors associated with our $^{40}Ar/^{39}Ar$ ages are estimates of the analytical precision at the 67% confidence level (1 $\sigma$) and include the precision error (0.5%) in the fluence-calibration parameter ($J$) but do not include the interlaboratory difference in fluence-monitor calibrations. Plateau ages are the weighted means and weighted standard errors (SE) of the plateau increments, where weighting is by the inverse of the variance (*23*). The ages were calculated with decay constants recommended in (*24*).

Four incremental heating and 23 total fusion $^{40}Ar/^{39}Ar$ ages were measured on single tektites in our Menlo Park laboratory with a continuous-laser $^{40}Ar/^{39}Ar$ dating system (*20, 25*). Another incremental heating age was measured in our Denver laboratory on a bulk sample of about 50 tektites (67 mg) with a resistance furnace, extraction line, and rare-gas mass spectrometer (*26*).

In the Menlo Park laboratory, the irradiated tektites, HC bentonite sanidine, and neutron-fluence monitors were loaded into wells in a copper planchet and placed in the sample chamber of the laser system. For the incremental heating measurements, individual tektites (0.8 to 1.2 mm, 0.9 to 1.2 mg) were progressively heated for 60 s per increment with a broadened (defocused) laser beam directed at the tektite through the sapphire window of the sample chamber. Temperature gradients within small samples heated in this way are negligible (*27*). At and below 1200°C, the sample temperature was measured with an infrared microscopic radiometer. It operates in the wavelength band of 1.0 μm to 5.8 μm and measures temperature relative to an internal blackbody cavity over an area (0.035 mm diameter) of the sample surface. The radiometer was malfunctioning above 1200°C, so we controlled the gas release at higher temperatures by increasing incrementally the power setting of the laser. Because the radiometer is used only to help control the fractional gas release, the malfunction had no effect on the resulting ages calculated from the incremental heating measurements. The gas released from the samples at each temperature step was cleaned with Zr-Al and Zr-V-Fe getters and analyzed with an ultraclean, ultrasensitive, rare-gas mass spectrometer.

We determined laser total fusion $^{40}Ar/^{39}Ar$ ages by melting individual tektites and small groups (two to ten grains) of monitor minerals and measuring the Ar released by the fusion. During the total fusion measurements, the tektites, sanidine, and hornblende were held for about 60 s at the maximum temperature achievable, estimated to be about 1500°C. The amount of radiogenic $^{40}Ar$ in all measurements exceeded 90%.

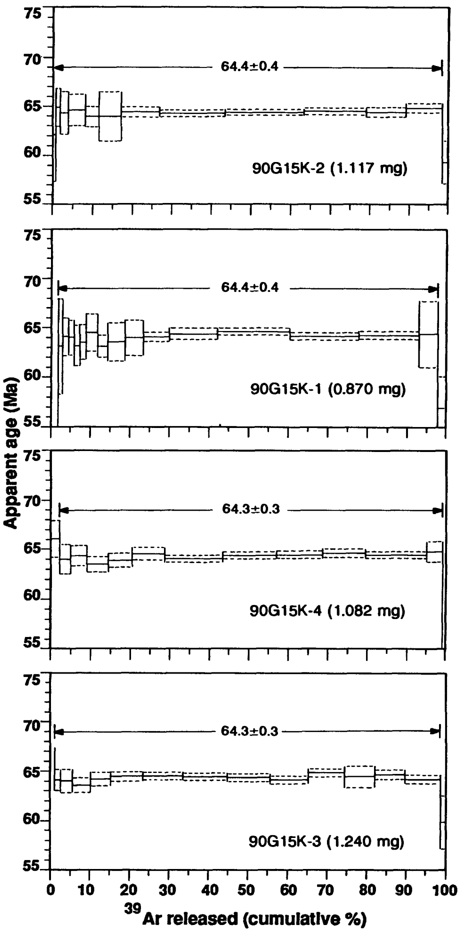

**Fig. 2.** Incremental heating $^{40}Ar/^{39}Ar$ age spectra of four tektites measured with the continuous-laser system. The mean of the four plateau ages is 64.38 ± 0.18 Ma.

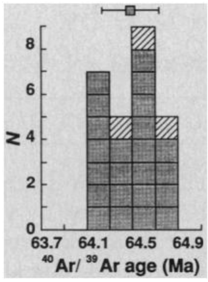

**Fig. 3.** Histogram showing results of 23 laser total fusion $^{40}Ar/^{39}Ar$ age determinations on Haitian K-T boundary tektites (stippled boxes) and three sanidine laser total fusion $^{40}Ar/^{39}Ar$ ages of the HC bentonite from Montana (hatched boxes). The bar at the top shows the simple mean and standard deviation of the tektite ages ($\bar{x}$ = 64.48 ± 0.22 Ma).

The four $^{40}Ar/^{39}Ar$ age spectra of the individual Haitian tektites determined with the laser system are essentially flat (Fig. 2 and Table 1) and show no evidence of disturbance after solidification. The $^{39}Ar/^{37}Ar$ ratios of the increments, as a function of the $^{39}Ar$ released, are also relatively constant, which is consistent with the behavior expected for a chemically homogeneous glass. The plateau for each of the four age determinations extends over 95% of the $^{39}Ar$ released. The four plateau ages are concordant with a weighted mean age of 64.38 ± 0.18 Ma (1 SE).

The $^{40}Ar/^{39}Ar$ age spectrum (13 steps) of the bulk sample of tektites measured with a resistance furnace has considerable dispersion in the lower temperature steps. However, the four high-temperature steps, which contain about 55% of the Ar released, form a plateau with a mean age of 65.6 ± 0.7 Ma (1 $\sigma$), using an age of 520.4 Ma for the MMhb-1 fluence monitor. If an age of 513.9 Ma were used for MMhb-1, as in the Menlo Park laboratory, the calculated plateau age would be 64.8 ± 0.7 Ma, which is not significantly different from the mean of the four laser-fusion plateau ages at the 95% level of confidence.

The 23 total fusion $^{40}Ar/^{39}Ar$ ages on single tektites (Fig. 3) acquired with the laser system range from 64.14 to 64.80 Ma, a difference of about 1.0%. They have a weighted mean of 64.48 ± 0.08 Ma (1 SE), which is not different from the laser incremental heating ages at the 95% level of confidence; the simple mean and standard deviation are 64.48 ± 0.22 Ma. The laser total fusion age measurements are inherently more precise than the laser incremental heating ages because the gas samples for the Ar isotopic analyses for the total fusion ages for are larger than the individual gas increments in the incremental heating analyses. Moreover, the lack of dispersion in the age spectra of individual tektites demonstrates that the total fusion ages are reliable solidification ages for the glass. Accordingly, we consider the weighted mean of the total fusion ages, 64.48 ± 0.08 Ma, to best represent the age of the Haitian tektites.

The three laser total fusion ages (Fig. 3) of sanidine crystals from the HC bentonite have a weighted mean of 64.57 ± 0.23 Ma (1 SE), which is not significantly different from the mean of the laser total fusion ages of the 23 individual tektites at the 95% level of confidence; the simple mean and standard deviation are 64.56 ± 0.16 Ma.

Our weighted mean total fusion $^{40}Ar/^{39}Ar$ age for the Haiti tektites (64.48 ± 0.08 Ma) and sanidine (64.57 ± 0.23 Ma) from the HC bentonite in Montana are consistent with conventional sanidine K-Ar ages from the HC bentonite (64.6 ± 0.5 Ma, 1 $\sigma$) and two other K-T boundary bentonites (64.8 ± 0.7 Ma and 65.8 ± 0.6 Ma, 1 $\sigma$) from Canada reported in (*9*). These authors reported a grand mean K-Ar age for biotite and sanidine (11 determinations) from the HC bentonite at 64.7 ± 0.6 Ma. Rb-Sr (biotite and feldspar) and U-Pb (zircon) ages reported by them for the bentonites are also concordant with our $^{40}Ar/^{39}Ar$ age determinations on tektites and sanidine. An older $^{40}Ar/^{39}Ar$ age of 66.0 ± 0.3 Ma (1 $\sigma$) for a split of the HC bentonite sanidine was determined in 1984 in the U.S. Geological Survey laboratory in Reston, Virginia (*8*), with an MMhb-1 age of 519.5 Ma (*28*). Recalculated with the Menlo Park value of 513.9 Ma for MMhb-1, this age is 65.3 ± 0.3 Ma, which is 1% higher than, and statistically different (95% confidence level) from, our age for the HC bentonite sanidine (64.6 Ma).

The Haitian tektites are the first datable impact products found in association with the worldwide Ir anomaly, and thus their age directly dates the time of the K-T impact or impacts. Our best $^{40}Ar/^{39}Ar$ age for these tektites is 64.5 ± 0.1 Ma, based on an age of 513.9 Ma for MMhb-1 (or 65.2 ± 0.1 Ma, using 520.4 Ma for the age of MMhb-1). Improvement in this value will require a more accurate age for neutron-fluence monitor minerals. Our new ages for the Haitian tektites and sanidine from the HC bentonite also show that the rocks deposited at the K-T boundary in both marine and continental environments are coeval at 64.5 ± 0.2 Ma.

Currently, the rocks at two known impact structures and another possible impact structure are being evaluated for lithologic, geochemical, and geochronologic evidence that might link them to the impact or impacts at the close of the Cretaceous Period. These include the Manson and Popigay impact structures in Iowa (*29*) and northcentral Siberia (*30*), respectively, and the Chicxulub structure, of possible impact origin, on the Yucatan platform (*10*, *15*). The Manson structure has been proposed as a possible K-T impact site for a variety of reasons (*31*). The $^{40}Ar/^{39}Ar$ age of shock-metamorphosed microcline (65.7 ± 1.0 Ma, using 520.5 Ma for MMhb-1) from granitic rock of the central uplift of the structure (*32*) suggested that the Manson impact was coeval with the K-T boundary. The age of 65.7 Ma for the Manson structure is indistinguishable statistically from our $^{40}Ar/^{39}Ar$ age of the K-T boundary tektites.

New $^{40}Ar/^{39}Ar$ ages of glass from the Popigay impact structure show considerable dispersion but suggest that it might be 64 to 66 Ma rather than 30 to 40 Ma, as previously thought (*33*). More $^{40}Ar/^{39}Ar$ ages and, particularly, fission-track ages of Popigay impact glass must be determined before its K-T boundary age can be accepted. An isotopic age for the Chicxulub structure has not been determined, although its stratigraphic age seems to be near the K-T boundary (*15*, *16*).

It is known that the K-T boundary occurred at a time when Earth's magnetic field was reversed, polarity Chron 29R, which lasted for about 0.5 million years (*34*). If, like the Manson structure, the Chicxalub and Popigay structures are shown to be coeval with the K-T boundary and mineralogically compatible with K-T boundary impact products, it follows that they must have formed during Chron 29R, and reversed remanent magnetism should be found in the rocks of their impact-melt sheets.

---

### REFERENCES AND NOTES

1. G. A. Izett, F. J-M. R. Maurrasse, F. E. Lichte, G. P. Meeker, *U.S. Geol. Surv. Open-File Rep. 90-635* (1990).
2. H. Sigurdsson *et al.*, *Nature* **349**, 482 (1991).
3. L. J. Spencer, *ibid.* **131**, 117 (1933).
4. K-Ar and $^{40}Ar/^{39}Ar$ ages for four other tektite groups using decay constants in (*24*) are as follows: (i) North American, $^{40}Ar/^{39}Ar$ ages of 35.4 ± 0.3 Ma [B. P. Glass, C. M. Hall, D. York, *Chem. Geol.* **59**, 181 (1986)] and 35.5 ± 0.3 Ma and $^{40}Ar/^{39}Ar$ age of 15.2 ± 0.2 Ma [J. D. Obradovich, L. W. Snee, G. A. Izett, *Geol. Soc. Am. Abstr. Programs* **21**, A134 (1989)]; (ii) moldavites, K-Ar age of 14.6 ± 0.2 Ma (*35*); (iii) Ivory Coast, K-Ar age of 1.3 Ma [W. Gentner, B. Kleinmann, G. A. Wagner, *Earth Planet. Sci. Lett.* **2**, 83 (1967)]; (iv) australite cores, mean K-Ar age of 0.88 ± 0.06 Ma (*35*), and australasian tektites, mean of 15 unpublished $^{40}Ar/^{39}Ar$ ages of 0.82 ± 0.07 Ma (G. A. Izett and J. D. Obradovich, unpublished data).
5. L. W. Alvarez, W. Alvarez, F. Asaro, H. V. Michel, *Science* **208**, 1095 (1980); W. Alvarez and F. Asaro, *Sci. Am.* **263**, 78 (October 1990).
6. B. F. Bohor and G. A. Izett, *Lunar Planet. Sci.* **XVIII**, 68 (1986); G. A. Izett, *Geol. Soc. Am. Bull.* **98**, 78 (1987).
7. R. E. Folinsbee, H. Baadsgaard, J. Lipson, *Ann. N. Y. Acad. Sci.* **91**, 352 (1961); M. Shafiqullah, R. E. Folinsbee, H. Baadsgaard, G. L. Cumming, J. F. Lerbekmo, *Int. Geol. Congress, 1964, Rep. XXII Session*, New Delhi, 1964, part 3, section 3, pp. 1–20; W. B. Harland, A. G. Smith, B. Wilcock, Eds., *Q. J. Geol. Soc. London Suppl.* 120s (1964); W. B. Harland and E. H. Francis, *Geol. Soc. London Spec. Publ. 5* (1971), part 1; J. D. Obradovich and W. A. Cobban, *Geol. Assoc. Can. Spec. Pap. 13* (1975), p. 31; J. F. Lerbekmo, M. E. Evans, H. Baadsgaard, *Nature* **279**, 26 (1979).

8. J. D. Obradovich, *27th Int. Geol. Congress Proc. 1,* (1984), pp. 11–30.
9. H. Baadsgaard, J. F. Lerbekmo, I. McDougall, *Can. J. Earth Sci.* **25**, 1088 (1988).
10. A. R. Hildebrand and W. V. Boynton, *Science* **248**, 843 (1990).
11. F. J-M. R. Maurrasse, *Survey of the Geology of Haiti, Guide to Field Excursions in Haiti,* Haiti, 3 to 8 March 1982 (Miami Geological Society, Miami, 1982).
12. G. Baker, in *Tektites,* J. A. O'Keefe, Ed. (Univ. of Chicago Press, Chicago, 1963), pp. 1–24.
13. F. J-M. R. Maurrasse, in *Trans. 1er Coll. Géol. d'Haiti,* Port-au-Prince, 27 to 29 March 1980 (Bureau of Mines and Energy Resources, Port-au-Prince, 1982), p. 184.
14. G. A. Izett, *Lunar Planet. Sci.* **XXII**, 625 (1991).
15. G. T. Penfield and A. Camargo Z., *Abstr. Soc. Econ. Geol. 51st Annu. Conv.* **1981**, P2.7 (1981); *Lunar Planet. Sci.* **XXII**, 1051 (1991).
16. V. L. Sharpton *et al., Lunar Planet. Sci.* **XXII**, 1223 (1991).
17. J. D. Obradovich provided us with a split of a sanidine concentrate sent to him by H. Baadsgaard.
18. The tektites, sanidine crystals from the HC bentonite, and three neutron fluence-monitor minerals were packaged in small, aluminum-foil packets and encapsulated in two quartz vials. One of the quartz vials contained a packet of 32 tektites. Individual tektites ranged from 0.5 to 1.3 mm in diameter and weighed from 0.3 to 1.2 mg. Another packet contained 31 mg of sanidine crystals ($\sim$150 μm) from the HC bentonite. The tektites and HC sanidine were sandwiched between packets of FCT sanidine, one of the fluence monitors. The vial also contained a packet of TCR sanidine and a second packet of MMhb-1 hornblende, the other two fluence monitors. The second vial contained a packet of about 50 tektites (67 mg) sandwiched between packets of fluence-monitor standards TCR sanidine and MMhb-1 hornblende. The samples were irradiated in the core of the U.S. Geological Survey's TRIGA reactor for 20 hours, where they received a fast neutron dose of $1.4 \times 10^{18}$ nvt.
19. G. B. Dalrymple, E. C. Alexander, M. A. Lanphere, G. P. Kraker, *U.S. Geol. Surv. Prof. Pap. 1176* (1981).
20. G. B. Dalrymple and W. A. Duffield, *Geophys. Res. Lett.* **15**, 463 (1988).
21. M. A. Lanphere, G. B. Dalrymple, R. J. Fleck, M. S. Pringle, *Eos* 71, 1658 (1990).
22. S. D. Samson and E. C. Alexander, *Chem. Geol.* 66, 27 (1987). The K and Ar measurements from the 18 laboratories have dispersions of 3.3 and 6.5%, respectively.
23. J. R. Taylor, *An Introduction to Error Analysis* (University Science Books, Mill Valley, CA, 1982) p. 270.
24. R. H. Steiger and E. Jäger, *Earth Planet. Sci. Lett.* **36**, 359 (1977).
25. G. B. Dalrymple, *U.S. Geol. Surv. Bull. 1890* (1989).
26. R. G. Tysdal, R. A. Zimmerman, A. R. Wallace, L. W. Snee, *U.S. Geol. Surv. Bull. 1922* (1990).
27. C. M. Hall, *Eos* 71, 653 (1990).
28. E. C. Alexander, G. M. Michelson, M. A. Lanphere, *U.S. Geol. Surv. Open-File Rep. 78-701* (1978).
29. R. R. Anderson and J. B. Hartung, *Lunar Planet. Sci.* **XXII**, 25 (1991).
30. V. L. Masaytis, M. V. Mikhaylov, T. V. Selivanovskaya, *Popigayskiy Meteoritnyy Krater* (Nauka, Moscow, 1975), p. 124. "Popigay" is the spelling used in a translation [*National Aeronautics and Space Administration Technical Translation F-16900* (1976)] of the foregoing report.
31. B. M. French, *Science* **226**, 353 (1984); G. A. Izett and C. L. Pillmore, *Eos* **66**, 1149 (1985); G. A. Izett, *U.S. Geol. Surv. Open-File Rep. 87-606* (1987); thesis, University of Alaska (1988); *Geol. Soc. Am. Spec. Pap. 249* (1990).
32. M. J. Kunk, G. A. Izett, R. A. Haugerud, J. F. Sutter, *Science* **244**, 1565 (1989).
33. A. L. Deino, J. B. Garvin, S. Montanari, *Lunar Planet. Sci.* **XXII**, 297 (1991).
34. E. M. Shoemaker, C. L. Pillmore, E. W. Peacock, *Geol. Soc. Am. Spec. Pap.* **209**, 131 (1987).
35. I. McDougall and J. F. Lovering, *Geochim. Cosmochim. Acta* **33**, 1057 (1969); T. Staudacher *et al., J. Geophys.* **51**, 1 (1982).

11 February 1991; accepted 30 April 1991

---

# Light-Transparent Phase Formed by Room-Temperature Compression of Graphite

WATARU UTSUMI AND TAKEHIKO YAGI

**Single-crystal graphite has been compressed at room temperature and found to undergo a transformation at 18 gigapascals as indicated by a drastic increase in the optical transmittance. This high-pressure phase is unquenchable; a more transparent phase formed by the heating of this phase can be quenched at ambient conditions. This latter phase is probably "hexagonal diamond," and the present observations suggest that the structure of the transparent phase obtained by the room-temperature compression is different from the hexagonal diamond structure.**

ALTHOUGH EXTENSIVE STUDIES have been carried out on diamond made by the catalyst-solvent process, little is known about the direct transformation from graphite to diamond under high pressure. More than 20 years ago, Aust and Drickamer (*1*) and Bundy and Kasper (*2*) found a sudden increase in the electrical resistivity of graphite when it was compressed above 15 GPa at room temperature. This change was reversible on release of pressure. When the sample was heated under pressure, however, a permanent increase in resistivity was observed, even after the complete release of pressure, and the "hexagonal diamond" phase was the phase in the recovered sample.

Recently, experiments have been carried out to investigate the behavior of natural single crystals of graphite at high pressure and room temperature. Hanfland *et al.* (*3, 4*) obtained Raman and reflectivity data and reported that the broadening of the high-frequency $E_{2g}$ Raman line and the decrease in optical reflectivity started at about 9 GPa, which indicated the onset of the transformation. This transformation was fully achieved at about 17 GPa. They stated that this transformation at room temperature may be related to the formation of an $sp^3$ bonded structure. On the other hand, Goncharov *et al.* (*5*) observed in the pressure range between 15 and 35 GPa a sharp decrease in the reflectivity and a simultaneous broadening of the intralayer Raman spectral band. They also reported that, with increasing pressure, the sample became transparent gradually from 35 GPa and eventually became light-transparent (bleaching effect) at about 55 GPa. They attributed these changes to the phase transformation into an amorphous phase. Moreover, Zhao and Spain (*6*) carried out powder x-ray diffraction experiments and reported that some new diffraction peaks appeared above 11 GPa but they could not identify the structure.

These experimental results indicate the possibility of a pressure-induced transformation in graphite at room temperature, but the nature and the pressure of this transformation remain unclear. In order to clarify these points, we carried out optical observations with single-crystal synthetic graphite.

A single crystal of kish graphite (Toshiba Ceramics Co.), which was formed by the supersaturation of carbon in molten iron, was used as a starting material. This sample was easily cleaved with a razor edge, and we prepared a very thin hexagonal-shaped single crystal ($\sim$1 μm thickness and 150 μm edge length). The experiments were carried out with a modified Mao-Bell–type diamond anvil cell, and the pressure was determined by the ruby fluorescence method. A mixture of methanol and ethanol (4:1) was used as the pressure medium.

Before the compression (Fig. 1A), because the sample was very thin, it was not completely opaque even at atmospheric pressure. When the pressure was increased at room temperature, visual observation in the pressure range below 18 GPa revealed no noticeable change. However, at 18 GPa, several light-transparent spots suddenly appeared in the sample (Fig. 1B), and they spread over the whole sample area while the pressure was kept constant. Figure 1C was taken 30 min and Fig. 1D 2 hours after the transformation had started. In each spot, the color change was not gradual but was discontinuous and drastic. On release of the pressure, the transparent phase reversed suddenly to the original dark-color phase at 2.5 GPa; thus, the high-pressure phase could not be quenched at ambient conditions.

Absorption spectra of the sample were measured under various conditions, and no noticeable structure was found in the visible light spectra. The pressure variation of the optical density at 580 nm is plotted in Fig. 2 for both increasing and decreasing pressure. This transition is reversible with large hysteresis. The optical density of the recovered sample is slightly higher than that of the starting material, probably because of the polycrystalline nature of the recovered material.

---

Institute for Solid State Physics, University of Tokyo, Roppongi, Minato-ku, Tokyo 106, Japan.